Validation of Atmospheric Precipitable Water in Three Reanalysis Products using Ground-based GPS Measurements

Junhong Wang[1] and Liangying Zhang[1]
Earth Observing Laboratory, NCAR, P. O. Box 3000, Boulder, CO 80307, U. S. A.
Correspondence: junhong@ucar.edu

INTRODUCTION

Global atmospheric reanalysis products have played an important role in current climate assessment, diagnostic studies of climate features, seasonal prediction, and climate predictability. Therefore, the validations of the reanalysis products are crucial for improving their accuracy and enhancing their applications. However, it is hard to find independent data with high quality and accuracy for the validations because most of datasets are assimilated by the reanalyses. Main outstanding issue in reanalysis as raised by the Intergovernmental Panel on Climate Change (IPCC, Trenberth et al. 2007) is the inhomogeneity of input data (both in-situ and satellite). Although various bias corrections have been applied to the input data, they remain imperfect.

The current reanalysis still has difficulty in simulating the hydrological cycle (e.g., Trenberth and Guillemot 1998). For instance, all three current reanalysis products (NCEP/NCAR, ERA-40 and JRA-25) overestimate global mean precipitation by more than 10% (Fig. 7 in Onogi et al. 2007). Previous studies also found that the reanalyses are deficient in reproducing the variability and trends of atmospheric precipitable water (PW), especially over the tropical oceans (e.g., Allan et al. 2004; Sudradjat et al. 2005; Trenberth et al. 2005). The conventional surface and radiosonde, and satellite observations are all assimilated into the reanalyses. Therefore, other independent PW data are needed. A global, 2-hourly PW dataset has been created from ground-based GPS measurements (Wang et al. 2007). This dataset has various scientific applications, including monitoring the quality of radiosonde humidity data and studying PW diurnal variations (Wang et al. 2007; Wang and Zhang 2008a and 2008b). The advantages of GPS-derived PW include the availability under all weather conditions, high accuracy (< 3 mm), high temporal resolution (5 min to 2-hourly) and, more importantly, its long-term stability. All of these make the GPS PW dataset appealing for validating the reanalysis PW data. In additional, none of the reanalysis products uses the GPS-PW data, which makes it an independent dataset for validations. This study evaluates the PW data from three reanalysis products (NCEP/NCAR, ERA-40 and JRA-25) by comparing with the 2-hourly GPS PW dataset from diurnal to decadal time scales.

RESULTS

In this study we use the six-hourly PW data from NCEP/NCAR (NNR), ERA-40 and JRA-25 reanalysis products (Kalnay et al. 1996; Uppala et al. 2005; Onogi et al. 2007). The ERA-40 and JRA-25 have a T106 horizontal resolution (equivalent to ~1.125ºX1.125º), while the NNR is on a ~2.5ºX2.5º grid. We also use the NNR temperature and humidity profile data on the T62 (~1.875X1.875º) horizontal resolution and 28 hybrid vertical levels. The 2-hourly GPS PW data are available at ~370 International GNSS (Global Navigation Satellite System) Service (IGS) stations around the globe from February 1997 to December 2006 and ~170 SuomiNet stations in U.S.A. from 2003 to 2006 (see Fig. 1 in Wang and Zhang 2008b). The following comparisons between the reanalyses (RAs) and the GPS data are made from February 1997 to December 2006 for NNR and JRA-25 at the IGS stations, from February 1997 to August 2002 for ERA-40 at the IGS stations, and from January 2003 to December 2006 for NNR and JRA-25 at the SuomiNet stations.

Direct comparisons

Geographic distributions of multi-year annual mean PW values are first compared among three reanalyses. The comparison shows some known features, the ERA-40's excessive water vapor in the tropics, the NNR's dry bias in the tropics and the NNR's wet bias over subtropical anticyclones (e.g., Trenberth et al. 2005). It also shows that the JRA-25 is drier than both NNR and ERA-40 over central Africa. Then the reanalyses and the GPS data are matched horizontally and temporally for direct comparisons. For the horizontal matching, the reanalysis grid boxes with GPS stations located inside are selected. For the temporal matching, two GPS data points close to the reanalysis time are averaged. For example, the reanalysis data point at 06 UTC is matched with the average of the GPS data points at 05 UTC and 07 UTC. Figure 1 shows the histogram of annual mean PW differences (RAs – GPS) at all stations. The NNR and JRA-25 are drier than the GPS data at over 70% of stations, while the ERA-40 has better agreement with the GPS data. One problem with this direct comparison is that the model surface height can be different from the GPS station height, and PW is very sensitive to the station elevation (Morland et al. 2006). The high correlations between the PW differences and the surface altitude differences in Fig. 2a confirm this. The surface altitude difference can be as much as ~3.5 km. The stations in the upper-left quarter in Fig. 2a are mainly island or coast mountainous stations, and the ones in the lower-right quarter are in the land high mountain regions where GPS stations are located near the foot of the mountains or in the valleys. There are two ways to limit this problem. One is to restrict the comparisons to the stations with the surface altitude differences less than 100 m. The histogram of annual mean PW differences at these stations in Fig. 2b still shows the negative bias in the NNR and JRA-25 at more than 70% of stations. Another way is to correct the surface altitude difference by calculating the layer PW from the GPS station ground to the model surface. The temperature and humidity profiles in the layer are interpolated or extrapolated from the reanalysis profiles using the similar method used in Wang et al. (2005, Fig. 1). The correction is applied to the NNR data. The correction has the largest impacts on the stations in the tails of Fig. 1 and changes the mode negligibly (not shown). There are still 71% of stations exhibiting drier NNR values after corrections. In conclusion, the direct comparison suggests that the NNR and JRA-25 have a negative bias in PW comparing with the GPS PW. More work needs to be done to find out where and when the dry bias is more profound and why it exists in the NNR and JRA-25.

Comparisons of PW diurnal variations

The diurnal cycle is one of the most obvious and reliable signals of the climate. However, there is a lack of data with high temporal resolution for studying the diurnal cycle on the global scale. The availability of the 2-hourly GPS PW data provides an unprecedented opportunity for us to study the water vapor diurnal variations and validate the reanalyses. The amplitude and phase of the PW diurnal cycle in U.S.A. and Europe are presented in Fig. 3 and 4, respectively, for the GPS data and three reanalysis products and for the Northern Hemisphere summer season (June-July-August). All four data sources show similar geographic patterns in amplitude in U. S. A., such as the larger amplitude over the Rockies, California, the low-level-jet region, and the east coast. The ERA-40 has the largest amplitude. The NNR has the best agreement with the GPS data in phase, showing the peaks from the late afternoon to early evening in the east, early morning over the Great Plains, and from 18 LST to 24 LST over the Rockies (Fig. 3). The JRA-25 is unable to reproduce the spatial variations of the diurnal phase and is dominated by the afternoon to the mid-night maximum over most of the U.S.A. The land-water contrast (Coast Ocean and lakes) in PW diurnal phase is pronounced in all reanalysis data.

The GPS data show the consistent phase at most of GPS stations (~12-20 LST) in Europe (Fig. 4). As a result, the diurnal cycle at all stations can be averaged to produce mean diurnal cycle in Europe (see Fig. 5). The PW diurnal amplitude is smaller in the NNR and JRA-25, especially in the South. The PW in the NNR and ERA-40 peaks several hours latter than the GPS PW. All three reanalyses again show the land-water contrast in phase, from the afternoon to night over land and in the morning over water. Seasonal variations of diurnal and sub-monthly PW variability in Europe are computed by averaging the data at all stations (Fig. 5). The diurnal anomalies are calculated from the fitted diurnal harmonics using derived amplitude and phase.

The GPS data shows that the PW diurnal cycle in Europe is strongest in summer with an amplitude of ~0.6 mm but weakest in spring; the local time of the maximum value makes a transition from early evening (~2000-2200 LST) in summer to late afternoon (~1600-1800 LST) in autumn and then to before noon (1000-1200 LST) in winter. The PW diurnal cycle is very weak and poorly represented in amplitude, phase and seasonal variation in the NNR and JRA-25. The ERA-40 has good agreement with the GPS data in summer, but fails to show the seasonal phase transition evident in the GPS data. The sub-monthly variability is much larger than the diurnal variation. That is not surprising because the sub-monthly variability is mainly a result of weather systems, whereas various competing factors can contribute to the diurnal variation. All three reanalysis datasets perform well in predicting sub-monthly variability and its seasonal and diurnal changes. Bock et al. (2007) found that the PW diurnal cycle is poorly represented in ERA-40 in Africa.

Comparisons in long-term variations

Thirteen GPS stations are found to have complete 10-year (1997-2006) PW record. Monthly mean PW anomalies at 13 stations from 1997 to 2006 from three reanalyses are well correlated with ones from the GPS dataset with correlation coefficients of larger than 0.8 at all stations except at MacQuarie Island. The time series show very good agreements on inter-annual variability among all four data sources. Among thirteen stations, three of them have nearby stations, so the comparisons between RAs or radiosondes and GPS are made (not shown). The PW differences between the radiosonde and the GPS show some known biases in radiosonde data and the discontinuities due to the changes of radiosonde types. The radiosonde biases are evident in RAs at one station, but not obvious at other two sites. The dry bias of Vaisala RS80-A data at MacQuarie Island can be as much as 20% and is consistent over the 10-year period, but it is not reflected in RAs. It is likely due to the small size (~35 km long and ~5 km wide) of the MacQuarie Island, and thus it is not well represented by the model grid box (> 100 km). The impact of the radiosonde bias on RAs depends on the weight of radiosonde data in RAs, differences in spatial representativeness between a point station and a grid box, and the contrary effects of biases from difference datasets.

CONCLUSIONS

The atmospheric precipitable water from NCEP/NCAR, ERA-40 and JRA-25 is evaluated by comparing with the PW data derived from the ground-based GPS measurements. The direct comparisons show that the NNR and JRA-25 have a dry bias at more than 70% of stations. The agreements between GPS and RAs in PW diurnal cycle vary from station to station. In U.S.A., GPS and RAs show similar patterns in amplitude, but NNR has the best agreement with GPS in phase. In Europe, NNR and JRA produces much weaker PW diurnal cycle; ERA-40 has consistent diurnal variations with GPS in summer, but fails to predict the seasonal transition of the diurnal phase. RAs have good agreement with GPS on sub-monthly variability and its diurnal and seasonal variations. RAs and GPS have very good agreements on PW inter-annual variability. The radiosonde humidity biases are not always evident in RAs. This study demonstrates that the global, 2-hourly GPS PW dataset is a valuable source for directly validating the reanalyses, helping homogenization of radiosonde humidity data for the reanalyses, and possibly using as an input data for RAs in the future.

REFERENCES

Allan, R. P., M. A. Ringer, J. A. Pamment and A. Slingo 2004: Simulation of the Earth's radiation budget by the European Centre for Medium-Range Weather Forecasts 40-year reanalysis (ERA40). J. Geophys. Res., **109**, D18107, DOI 10.1029/2004JD004816.

Bock, O., F. Guichard, S. Janicot, J. P. Lafore, M.-N. Bouin and S. Sultan 2007: Multiscale analysis of precipitable water vapor over Africa from GPS data and ECMWF analyses. Geophys. Res., Lett., **34**, L09705, doi:10.1029/2006GL028039.

Kalnay E. and Coauthors 1996: The NCEP/NCAR 40-year reanalysis project. Bull. Amer. Meteor. Soc., **77**, 437–471.

Morland J, M. A. Liniger, H. Kunz, I. Balin, S. Nyeki, C. Matzler, N. Kampfer 2006: Comparison of GPS and ERA40 IWV in the Alpine region, including correction of GPS observations at Jungfraujoch (3584 m). J. Geophys. Res., **111**(D04102). doi: 10.1029/2005JD006043

Onogi, K., J. Tsutsui, H. Koide, M. Sakamoto, S. Kobayashi, H. Hatsushika, T. Matsumoto, N. Yamazaki, H. Kamahori, K. Takahashi, S. Kadokura, K. Wada, K. Kato, R. Oyama, T. Ose, N. Mannoji and R. Taira 2007: The JRA-25 Reanalysis. J. Meteor. Soc. Japan, **85**, 369-432.

Sudradjat, A., R. R. Ferraro and M. Fiorino 2005: A comparison of total precipitable water between reanalyses and NVAP. J. Climate, **18**, 1790-1807.

Trenberth, K. E., and coauthors 2007: Observations: Surface and Atmospheric Climate Change. In: Climate Change 2007. The Physical Science Basis. Contribution of WG 1 to the Fourth Assessment Report of the Intergovernmental Panel on Climate Change. [S. Solomon, D. Qin, M. Manning, Z. Chen, M. C. Marquis, K. B. Averyt, M. Tignor and H. L. Miller (eds)]. Cambridge University Press. Cambridge, U. K., and New York, NY, USA, 235–336.

Trenberth, K. E., and C. J. Guillemot 1998: Evaluation of the atmospheric moisture and hydrological cycle in the NCEP/NCAR reanalyses. Climate Dyn., **14**, 213-231.

Trenberth, K. E., J. Fasullo and L. Smith 2005: Trends and variability in column-integrated water vapor. Clim. Dyn., **24**, 741-758.

Uppala, S. M. and coauthors 2005: The ERA-40 reanalysis. Quart. J. Roy. Meteor. Soc., **131**, 2961-3012.

Wang, J., L. Zhang, A. Dai, T. Van Hove and J. Van Baelen 2007: A near-global, 2-hourly data set of atmospheric precipitable water from ground-based GPS measurements. J. Geophys. Res., **112**, D11107. doi;10.1029/2006JD007529.

Wang J. and L. Zhang 2008a: Systematic errors in global radiosonde precipitable water data from comparisons with ground-based GPS measurements. J Climate, in press.

Wang, J. and L. Zhang 2008b: Climate applications of a global, 2-hourly atmospheric precipitable water dataset from IGS ground-based GPS measurements, J. of Geodesy, submitted.

Wang, J., L. Zhang and A. Dai 2005: Global estimates of water-vapor-weighted mean temperature of the atmosphere for GPS applications. J. Geophys. Res., **110**, D21101, doi:10.1029/2005JD006215.

ACKNOWLEDGEMENTS

This work was supported by a NOAA grant (No. NA06OAR4310117). We would like to thank Kevin Trenberth and Aiguo Dai (both at NCAR) for useful comments. The National Center for Atmospheric Research is sponsored by the U.S. National Science Foundation.

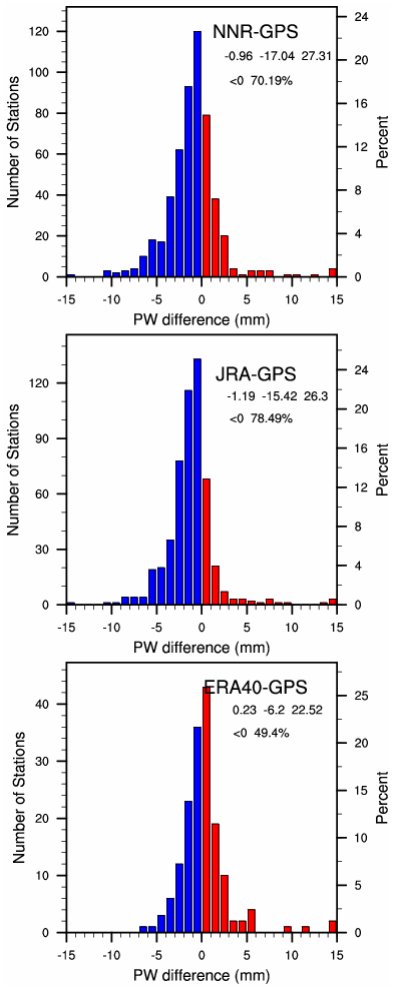

Fig. 1 Histograms of annual mean PW differences at all stations. The mean, minimum and maximum values, and the percentage of stations with negative PW differences are given in the legend.

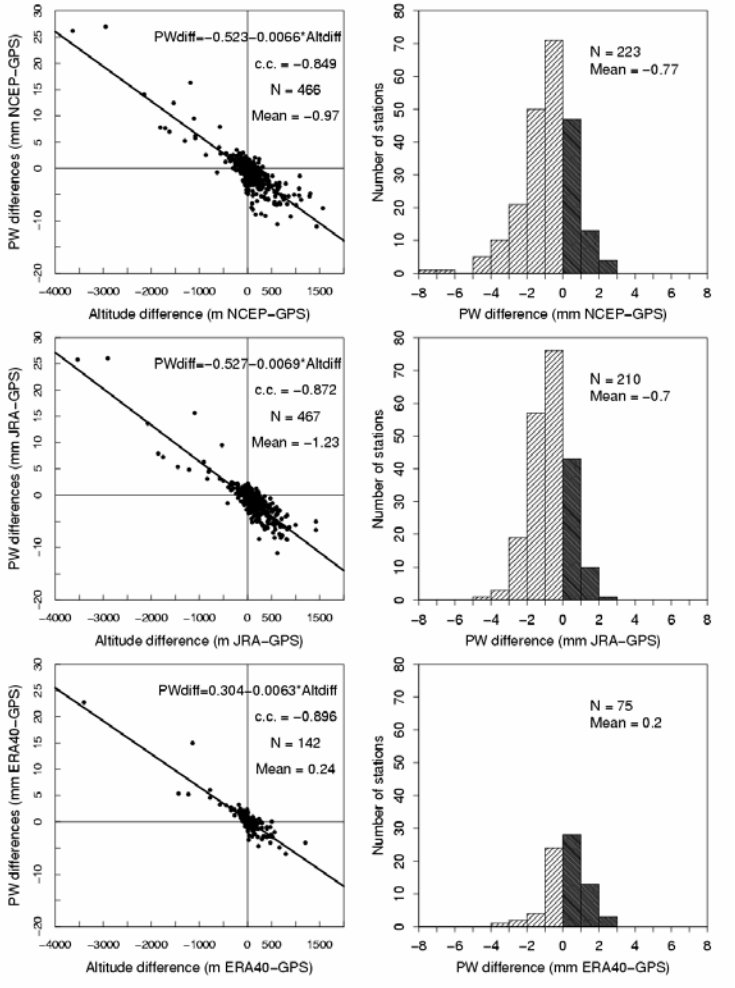

Fig. 2. The left panel shows the scatter plots of annual mean PW differences versus the surface altitude differences. The right panel is the histogram of annual mean PW differences only for stations with the surface altitude differences less than 100 m.

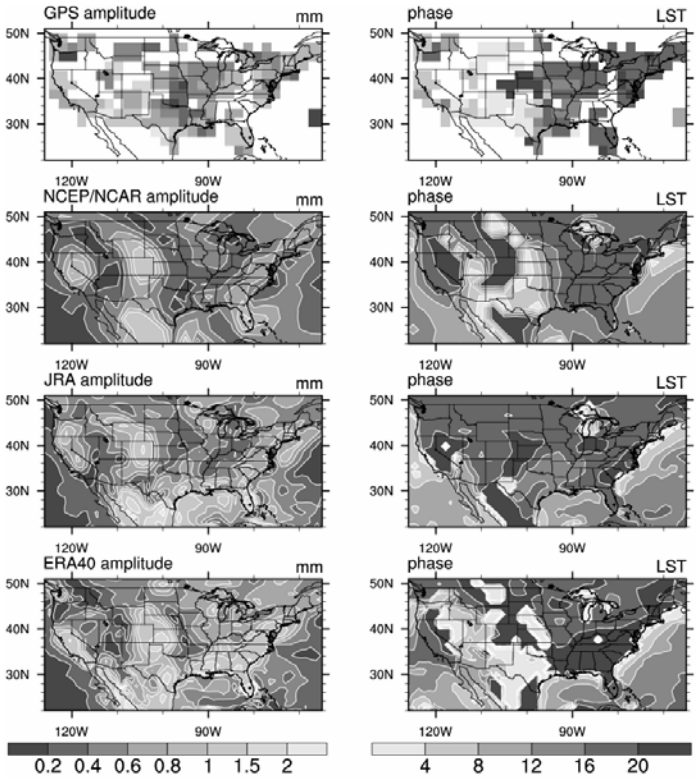

Fig. 3 Spatial distribution of the amplitude (mm, left panel) and phase (LST, right panel) of the diurnal harmonic of JJA mean PW in U.S.A.

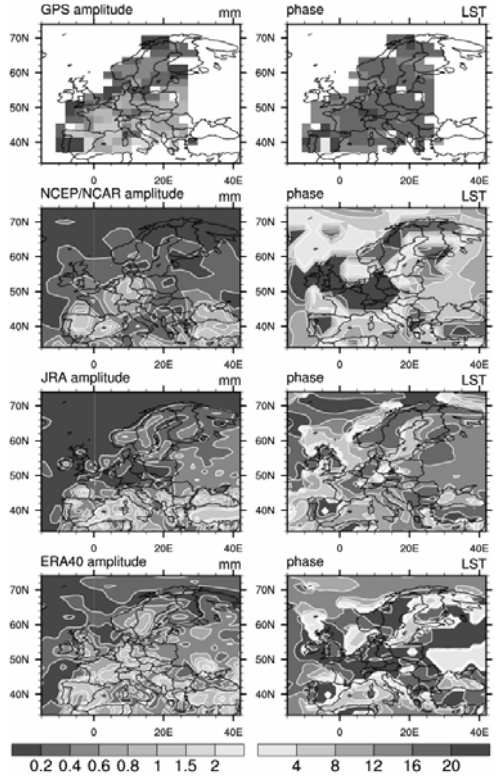

Fig. 4 Same as in Fig. 3 but for Europe.

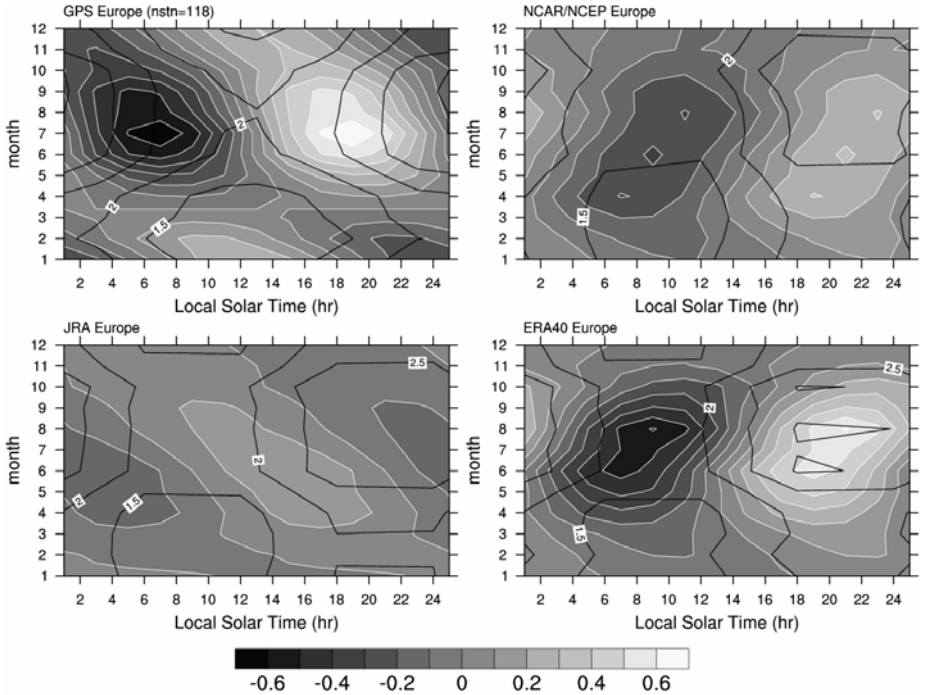

Fig. 5 Comparisons of seasonal variations of PW fitted diurnal anomalies (in mm, color) in Europe. The contours show the sub-monthly variability (mm).